Quantum Tunneling of Magnetization in Nanostructured Materials

J. Tejada*

Dept de Fisica Fonamental, Universitat de Barcelona, Diagonal 647, 08028 Barcelona, Spain

R. F. Ziolo

Wilson Center for Research and Technology, Xerox Corporation, Webster, New York 14580

X. X. Zhang

Dept de Fisica Fonamental, Universitat de Barcelona, Diagonal 647, 08028 Barcelona, Spain

Received March 20, 1996. Revised Manuscript Received June 6, 1996[⊗]

The study of very low temperature magnetic relaxation in nanostructured materials has provided the opportunity to observe the occurrence of quantum tunneling of magnetization (QTM) in many different systems. As the magnetization is a classical vector, this effect is also referred to as macroscopic quantum tunneling (MQT). In this paper, we review the key ideas underlying magnetic relaxation as well as the results obtained for different nanostructured systems, which, to date, include single domain particles, mesoscopic grains, and high-spin polynuclear molecules.

1. Introduction

One of the most interesting aspects of the behavior of a nanometer size magnet is the fact that the north and south magnetic poles may suddenly interchange due to quantum tunneling. In this case, the magnetic moment of the particle behaves as a quantum object rather than a classical vector,[1] and the phenomenon is referred to as quantum tunneling of magnetization (QTM). Similar effects include quantum nucleation of magnetic bubbles[1] and quantum depinning of domain walls from defects in bulk ferromagnets.[2] Since magnetization is a classical vector, the phenomenon is also referred to as macroscopic quantum tunneling (MQT). Familiar examples of the latter are Josephson junctions and SQUIDs.

Tunneling is a consequence of quantum mechanics, which states that an elementary particle, such as an electron, confined within a certain volume, may literally disappear from inside that volume and reappear outside of the volume. The tunneling microscope is an example of an application of such behavior.

The occurrence of quantum tunneling of magnetization was suggested as early as 1959 when Bean and Livingston[3] proposed an explanation of why particles in a sample of nickel powder failed to reach their blocking temperature down to 4.2 K.[4] It was not until the late 1980s, however, that progress began, when it was suggested theoretically that the quantum uncertainty in the position of the magnetic poles in a nanometer size magnet is large, making stabilization of the magnetic configuration impossible, irrespective of the temperature.[1] Thus, for such a particle, its state is a superposition of a "spin up" and "spin down" state as a consequence of the tunneling of the magnetic moment. Such behavior may have important consequences in determining the lifetime of magnetic information storage when using nanoscale magnets. Here, the magnetic moment of the nanometer particles would never block as a consequence of tunneling, which, in turn would limit the storage density. On the other hand, magnetic tunneling offers a very exciting possibility for computers using mesoscopic magnets for memory. In the presence of quantum tunneling, the memory unit of such a computer will be in a superposition of the spin-up (yes) and spin-down (no) states. The relative probabilities of "yes" and "no" will then depend on the history of the interactions of the memory units with the writing and reading processes. Magnetic tunneling is of fundamental importance, not only for potential information and computation applications but also because it presents the possibility to deal experimentally with a single quantum object of mesoscopic size.

Nanostructured materials, which incorporate mesoscopic magnets, constitute an important arena for the study of quantum tunneling of magnetization (QTM) and dissipation effects during the occurrence of quantum phenomena. In this paper, we present a brief review of the physics underlying the dynamics of the magnetic moment of mesoscopic particles, the use of low-temperature relaxation measurements, which constitute an ideal situation for the experimental observation of QTM, and the materials in which QTM has been observed. The latter include ferritin protein, nanoscale γ-Fe_2O_3 and $CoFe_2O_4$ particles, mesoscopic granular materials, and a high-spin polynuclear cluster compound of manganese.

2. Background Physics

The absolute minimum energy of a system of interacting single domain particles corresponds to a certain

[⊗] Abstract published in *Advance ACS Abstracts,* August 15, 1996.

S0897-4756(96)00200-1 CCC: $12.00

orientation of their individual magnetic moments. In experiments, however, this state is difficult to achieve because of the existence of metastable states which result in magnetic hysteresis and time-dependent phenomena. Metastable states in single domain particles are separated from each other by intrinsic energy barriers associated with anisotropy, which are of the order of $H_K MV$, where H_K is the effective anisotropy field, and M and V are the magnetization and volume of the particle, respectively.

In an applied magnetic field, the magnetic moment of a system composed of interacting particles with different volumes has a two-step evolution. The first rapid stage finishes when the system arrives at a critical state due to the balance of the magnetic driving force and the frictional force from the barriers. The second slow phase of the evolution, which is detected experimentally in the relaxation experiments, is due to thermal or quantum transitions in the presence of the energy barriers. Starting with zero barrier, the system automatically reaches a barrier for which the lifetime of the metastable states equals the observation time of the experiment. The universal signature of these slow relaxation processes is their ln(t) character. Though each individual metastable state decays exponentially with time, their cumulative effect transforms the exponential decay into the ln(t) dependence.

3. Physics Underlying the Dynamics of Magnetization

In the absence of a magnetic field, the energy of a particle is minimized when its magnetic moment coincides with the anisotropy axis. The two equivalent but opposite orientations of the magnetic moment are separated by an energy barrier, which scales linearly with the volume of the particle. In 1988, it was predicted[1] that at low temperature, the magnetic moment can quantum mechanically tunnel through the energy barrier with a probability exp($-B$). As the temperature rises, the thermal transitions dominate the energy barriers. The rate for this process is described by exp($-U/k_BT$), where U is the energy barrier. One can define a crossover temperature, $k_BT_C = U/B$, below which quantum under-barrier transitions dominate.

Therefore, for a collection of identical, noninteracting single domain particles aligned in the same direction by a field, the anisotropy energy barrier would be universal throughout the system. As the magnetic field is switched off, the magnetization of the system relaxes as

$$M(t) = M(0)\exp(-\Gamma t) \tag{1}$$

where Γ is the decay rate given by

$$\Gamma = \Gamma_0 \exp(-U/k_BT_{esc}(T)) \tag{2}$$

Here $T_{esc}(T)$ is called the escape temperature. For thermal transitions, $T_{esc}(T) = T$, while for quantum under-barrier transitions, $T_{esc}(T) =$ constant. Γ_0 is the attempt frequency and is on the order of 1 GHz. If the thermal fluctuation is much higher than the energy barrier, the magnetic moment oscillates rapidly between the two orientations. This situation corresponds to superparamagnetic behavior, wherein it is impossible to follow the relaxation process.

To observe the exponential relaxation in an array of single domain particles, one needs a very narrow distribution of particle sizes, because Γ depends exponentially on the volume of the particle. While it is very difficult to prepare such a system, fortunately, there are solids constituted by identical molecular blocks[5] in which it is possible to find an universal anisotropy barrier throughout the entire system.

Consider now a system at low temperature, composed of particles of different sizes having their anisotropy axes in different orientations with respect to the applied field. That means that we are considering a system with a broad distribution of energy barriers. If the field is suddenly removed or changed to a new value, H, the magnetization drops to a finite value determined by the hysteresis curve. The latter, slow phase of the evolution of the magnetization follows[6]

$$M(t) = M(t_0)[1 - S(T,H)\ln(t/t_0)] \tag{3}$$

Here $S(T,H)$ is called the magnetic viscosity and its dependence on temperature and magnetic field H characterizes the relaxation of the system. Let $U(H)$ be the average energy barrier, which determines the so-called blocking temperature, T_B, in the presence of the magnetic field H. T_B corresponds to the temperature at which the average relaxation time of the magnetic moments equals the experimental measuring time. In static measurements of the magnetization, this time is about 30 s, therefore $30 = 10^{-10}\exp(\langle U(H)\rangle/k_BT)$, which gives $25k_BT \cong \langle U(H)\rangle$. At $T > T_B$, the system behaves superparamagnetically, that is, no time effects occur, and, at $T < T_B$, the system is in the blocked state where the relaxation is logarithmic in time. It has been demonstrated[6] that for $T \ll T_B$, the magnetic viscosity can be expressed as

$$S(T) = k_BT/\langle U\rangle \tag{4}$$

When $M(t)$ is measured systematically in the temperature interval $T_C \le T \le T_B$, it is possible to analyze the data in terms of the unique variable $T\ln(\Gamma_0 t)$.[6,7] Although Γ_0 is weakly temperature dependent and, in complex systems, there is a distribution of Γ_0 values, the $T\ln(\Gamma_0 t)$ plot remains good, at low temperature, to a first-order approximation.

Recently, the physical picture of magnetic relaxation has been better understood through computer simulations of the relaxation in small magnetic single domain particles. The Monte Carlo method has been used[8] to study the magnetic relaxation of a set of 36 000 particles with a log-normal size distribution. It is assumed that for each particle the probability of transition between different orientations of the magnetic moment is exp($-U/k_BT$), where the energy barrier U is proportional to the volume of the particle. When all particles are identical, the relaxation is exponential as expected. When there is a size distribution and five different distributions were studied, the relaxation follows very well the ln(t) law in both cases of independent and interacting particles.

A different mathematical approach has also been used to study the problem.[9] In this case, the variation with time of the magnetization of an array of single domain

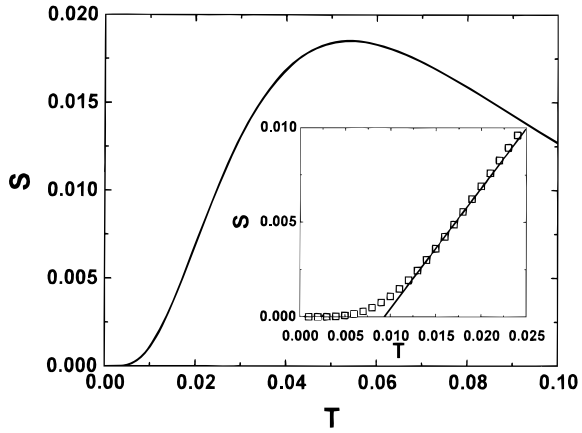

Figure 1. Computational magnetic viscosity $S(T)$ (=$(1/M_0)$dM/d(ln t)) deduced from the variation with the time of the magnetization of an array of single domain particles after changing the applied magnetic filed.[9] The inset is an expansion of the big figure.

particles is computed after changing the applied magnetic field from its initial value H_1 to a final value H_2:

$$M(t) = \frac{\int_0^\infty f(V)VM_S\{g(H_2) + [g(H_1) - g(H_2)]\exp(-t\Gamma(V))\}\,\mathrm{d}V}{\int_0^\infty Vf(V)\,\mathrm{d}V} \quad (5)$$

Here $M_S(T)$ is the saturation magnetization at each temperature, $M_S(T)/M(0) = 1 - (T/T_0)^{3/2}$, T_0 is the ordering temperature of the particles, $g(H)$ is the Brillouin function, and Γ is the relaxation rate $\Gamma = \Gamma_0 \exp[-U/k_BT_{esc}(T)]$, where the escape temperature, $T_{esc}(T)$, presents a temperature dependence characteristic of weak damping processes, $T_{esc}(T) = T_C \coth(T_C/T)$. The energy barrier $U = KV$ and the anisotropy constant K depend on the temperature as $K(T)/K(0) = [(M_S(T)/M(0)]^3$. In the computations, the volume distribution was assumed to be log-normal as $f(V) \propto \exp(-\log^2(V/V_m)/(2\sigma^2))$ where V_m is the average volume and σ is the distribution width.

From all of the studies (Figure 1), it has been well established that the temperature dependence of the magnetic viscosity, $S(T)$, shows the following universal features: (1) $S(T)$ never extrapolates to a positive nonzero value when only thermal processes are considered; that is, $T_C = 0$; (2) a plateau in the viscosity appears below T_C; (3) $S(T)$ increases nearly linearly with T at low temperature $T_C \leq T \ll T_B$; (4) at T near T_B, $S(T)$ loses its linear dependence on T and shows a maximum; (5) at $T \sim T_B$, where a major portion of the particles relax superparamagnetically, the time interval in which the relaxation follows the ln(t) dependence is reduced, and above T_B the viscosity decreases as the temperature increases; (6) when the field is increased during the relaxation process, both the maximum in viscosity and crossover temperature shift to lower temperatures as a consequence of the reduction in the energy barrier height; (7) the $S(T)$ curves for noninteracting and interacting particles show similar features.

4. Experimental Methodology

The objective of the relaxation experiments is to measure the slow decay of magnetization from the critical states developed after changing the magnetic field.[10,11] When the magnetic field acting on a magnetic system is changed suddenly from H_1 to H_2, the magnetization of intensity M_1 is changed to a new value, M_2. After a certain waiting period, which depends on the measuring technique being used, the variation of M_2 with time is recorded in a few hours. It has been estimated[12] that the self-heating phenomena associated with the fast and slow relaxation of the magnetization do not play any important role when the relaxation experiments are carried out in the kelvin regime.

5. Theoretical Considerations

In this section, we comment on the theoretical suggestions concerning both the crossover temperature T_C and the quantum tunneling rate for ferromagnetic mesoscopic particles or grains.[1] In this case, one should note that the crossover temperature, $T_C \approx (\mu_B/k_B)(H_{||}H_\perp)^{1/2}$ ($H_{||}$ is the easy anisotropy field and $H_\perp$ is the field responsible for the noncommutation of $M_{||}$ with the Hamiltonian), is a characteristic of the material and independent of the extensive parameters like the volume of the particle, although the tunneling rate has a very strong dependence on the size and decreases exponentially with the increasing particle volume. The fact that T_C scales with the magnetic anisotropy constant K (=$^1/_2H_{||}M_S$, where M_S is the saturation magnetization of the material) of the material may be easily verified using particles with different anisotropy. For $K = 10^7$ erg/cm^3, the crossover temperature should be of a few kelvin. When considering the tunneling volume, it is important to notice that the preexponential factor Γ_0, which enters in the relaxation rate given in eq 2, is of the order of 10^{10} s^{-1}. Thus, if one wants to observe quantum relaxation processes that take hours, the tunneling exponent B should not exceed 25. This, therefore, limits the volume and number of spins of the magnetic particles, $V = 25k_BT_C/K$. The size of the particles showing tunneling as well as the crossover temperature depends on the external applied field. When the external magnetic field is close to the anisotropy field H_K ($\equiv H_{||}$), one has to consider the reduction in the barrier heights, $U(H) = U(H=0)(1 - H/H_K)^2$, which allows one, in principle, to monitor the size of the particles that tunnel during the experimental time. T_C decreases as the applied field, H, increases.

For nanoscale antiferromagnetic particles, which have small noncompensated magnetic moments due to finite size effects, the crossover temperature T_C depends on the ratio between the anisotropy constant of the material and the magnetic susceptibility,[13] i.e., $k_BT_C \approx \mu_B\sqrt{K_{||}/\chi_\perp}$. Therefore, the materials with $K_{||} = 10^6$ erg/cm^3 and $\chi_\perp \leq 10^{-4}$, which can be matched in many different materials, should exhibit a crossover temperature above a few kelvin. The tunneling exponent $B = 25$, can be, in this case, matched by particles having larger sizes than that for ferromagnetic tunneling. Since the exponent $B_{AFM} \sim NS_0(H_{||}/H_{ex})^{1/2}$ for antiferromagnetic tunneling, and $B_{FM} \sim NS_0(H_{||}/H_\perp)^{1/2}$ for ferromagnetic tunneling (where N is the number of atoms in a grain, S_0 is the atomic spin, and $H_{||}$ and $H_\perp$ are the parallel and transverse anisotropy field of the materials), in general, $(H_{||}/H_{ex})^{1/2} \ll (H_{||}/H_\perp)^{1/2}$. Thus the antiferromagnetic grains could have more atoms than the ferromagnetic grains for satisfying $B = 25$.

Table 1. Summary of the Nanostructured Materials Studied for MQT and Their Associated Parameters[a]

material	av diam (nm)	H_K (kOe)	T_B (K)	T_C (K)	ref
Fe_3O_4	6	5	30	?	[23]
γ-Fe_2O_3 (in water)	5	5	140	?	[22]
γ-Fe_2O_3 (in silicate)	5	10	220	2.2	[22]
FeC	3.6	15	20	1	[27]
$CoFe_2O_4$ (in water)	3	50	170	2.5	[28]
$CoFe_2O_4$ (in silicate)	3	50	170	5	[28]
FeOOH	3		47	7	[26]
$NiFe_2O_4$	7	60	170	2	[24]
TbCeFe	15	60		0.6	[25]
CrO_2	100	12	500	4	[29]
$BaFe_{12}O_{19}$ platelet		20	160	3	[30]
ferritin	8	100	13	2.1	[16]

[a] For Fe_3O_4 and γ-Fe_2O_3 particles dispersed in water and oil, the crossover temperature has not yet been found. In any case, the experiments show that the crossover temperature should be lower than 1 K in accord with theoretical suggestions. H_K is the anisotropy field, which experimentally can be estimated from the field occurring irreversibility in the hysteresis loop.

6. QTM in Nanostructured Materials: Five Systems

Table 1 lists some materials in which QTM has been observed. Five of these systems are reviewed here that include mesoscopic particles of ferritin and ferrites, granular rare earths, and a polynuclear cluster compound.

6.1. Ferritin Protein. Ferritin is a giant clathrate consisting of a protein cage containing the biogenic mineral ferrihydrite combined with phosphate. The cage is a sphere of about 80 Å in diameter and is able to store up to 4500 Fe^{3+} atoms.[14] The Néel ordering temperature of the magnetic iron core of the ferritin is $T_N = 240$ K. Mössbauer studies of the protein show a well-defined magnetic sextet at 4.2 K, which, as the temperature is raised, changes into a doublet at 50 K.[15] This is consistent with the findings of Tejada et al. and of Gider et al. for a blocking temperature of about 13 K[16,17] and with the shifting of the blocking temperature with frequency in ac-field experiments.[18] The sample used in these experiments was commercial ferritin from horse spleen (Fluka Biochemika, 46230). The solution volume was 0.36 cm^3 and the protein concentration in the solution was 50 mg/cm^3. Therefore, the sample contained 1.2×10^{16} protein particles.

Zero field cooled (ZFC) and field cooled (FC) magnetization measurements were performed to observe the freezing of the Néel vector $\boldsymbol{l}$ defined as $\boldsymbol{l} = (\boldsymbol{M}_1 - \boldsymbol{M}_2)/2M_0$, where $M_0 = |\boldsymbol{M}_1| = |\boldsymbol{M}_2|$ is the modulus of the magnetization for the two ferromagnetic sublattices. As the Néel vector jumps through the barriers between $\boldsymbol{l}$ and $-\boldsymbol{l}$ states due to thermal or quantum transitions, the total noncompensated magnetization $\boldsymbol{M} = \boldsymbol{M}_1 + \boldsymbol{M}_2$ does so as well. This allows study of the dynamics of $\boldsymbol{l}$ by measuring the time dependence of the magnetization. The blocking of M at about $T_B = 13$ K, maximum in the ZFC curve, is ascribed to the blocking of $\boldsymbol{l}$. The broad peak at the blocking temperature indicates the existence of a broad distribution of energy barriers. Above T_B, the ZFC and FC curves follow the Curie−Weiss law with a superparamagnetic temperature of a few kelvin (Figure 2 and inset). From the Curie−Weiss law, we have estimated[16] that the average number of uncompensated surface spins per molecule is 15.

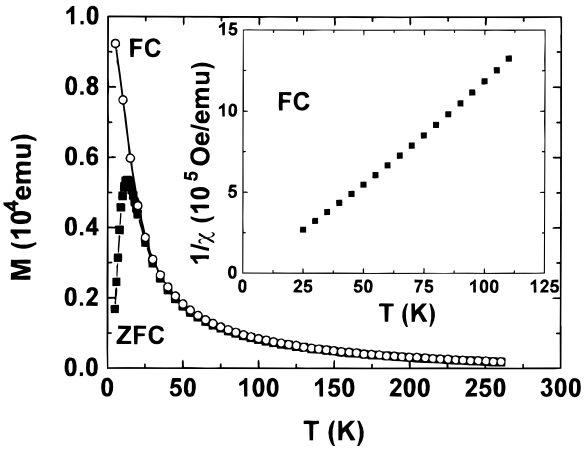

Figure 2. Temperature dependence of magnetization for protein molecules obtained in the zero field cooled (ZFC) and field cooled (FC) process with applied field $H = 0.01$ T. Inset: the inverse FC susceptibility versus temperature.

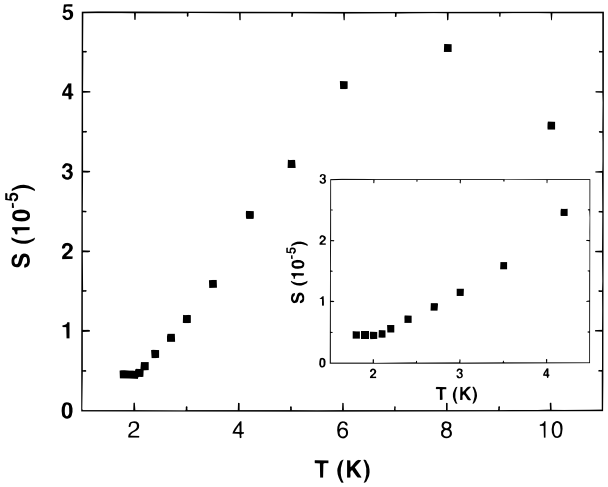

Figure 3. Magnetic viscosity extracted from the relaxation data as a function of temperature for the ferritin protein sample.

The relaxation experiments were performed following the procedure discussed above. The protein sample was cooled from 250 K to a target temperature in a field $H_1 = 0.01$ T, then the field was changed to $H_2 = -0.01$ T. The relaxation follows the ln(t) law as expected due to the broad distribution of metastable states as detected in the ZFC measurements. The extracted magnetic viscosity (Figure 3) exhibits the following features: $S(T)$ has a maximum at $T \sim T_B$, and it has also been found that in the relaxation data above T_B, the time interval in which $M \propto \ln(t)$ is reduced. This is in agreement with the interpretation of T_B as the temperature separating the superparamagnetic and blocked behavior of the Néel vector. $S(T)$ is independent of temperature below 2.1 K, indicating that $T_{esc}(T) =$ constant below this temperature. This suggests the occurrence of quantum tunneling underbarrier transitions for the Néel vector. The theoretical expectation for the crossover between the thermal and quantum regime is $k_B T_C \approx \mu_B \sqrt{K_{\parallel}/\chi_{\perp}}$. The order of magnitude of T_C can be estimated by using $K = 2.5 \times 10^5$ erg/cm^3 and $\chi_{\perp} \sim \chi = 20 \times 10^{-6}$ [19] to give $T_C = 3$ K, which is in good agreement with $T_C = 2.1$ K observed in these experiments.

The tunneling volume can be estimated from the expression of the B exponent,[13] where $B = (V/\mu_B)$-

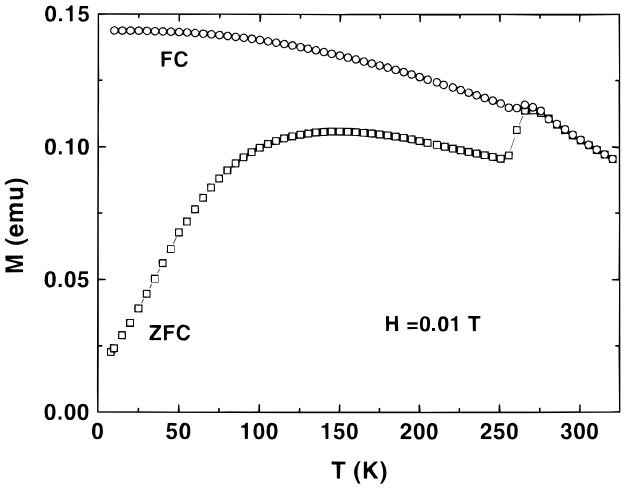

Figure 4. ZFC-FC magnetization as function of temperature for γ-Fe_2O_3 particles dispersed in water (as ferrofluid).

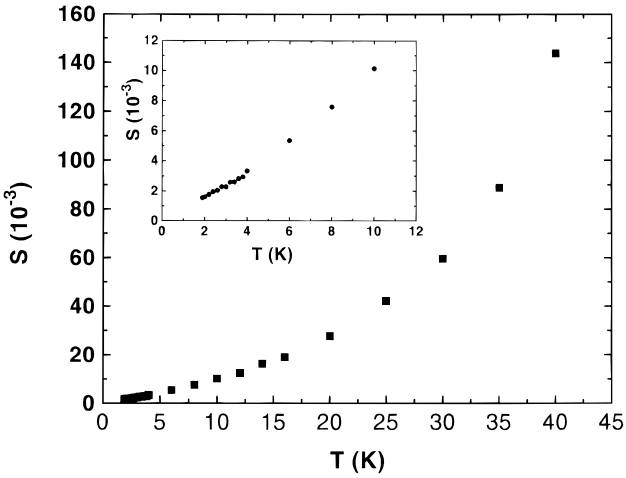

Figure 5. Temperature dependence of the magnetic viscosity for the γ-Fe_2O_3 ferrofluid. The inset shows the low-temperature data.

$(\chi_\perp H_{||})^{1/2}$, which, as discussed before, for our experimental time window, should be equal to 25. We have found that $V = 8 \times 10^4$ Å^3 corresponding to particles with a diameter smaller than 50 Å.

6.2. Nanoscale γ-Fe_2O_3 Particles Dispersed in Water. In Figure 4, we show the ZFC and FC magnetization curves for a sample of aqueous ferrofluid containing γ-Fe_2O_3 particles with a mean diameter of about 10 nm in sulfonated polystyrene.[20,21] The broad peak observed in the ZFC curve corresponds to a broad distribution of relaxation times for metastable states. The jump in the ZFC values at 273 K is due to transformation of ice to water, wherein the particles become free and align along the field.[22]

The magnetic relaxation data were obtained using the values of $H_1 = 0.01$ T and $H_2 = -0.01$ T. The remnant magnetization relaxes following the ln(t) law; the extracted magnetic viscosity data are shown in Figure 5. We have also found that the $M(t)$ data follow the T ln(t) plot throughout the entire temperature range used in the experiment (Figure 6). Both sets of data suggest that the relaxation of these particles is always thermally activated. The theoretical prediction for the crossover temperature to the quantum regime, with $H_K = 0.5$ T, is about 0.5 K, which is below our lowest temperature of 1.8 K. Similar results have been obtained for other

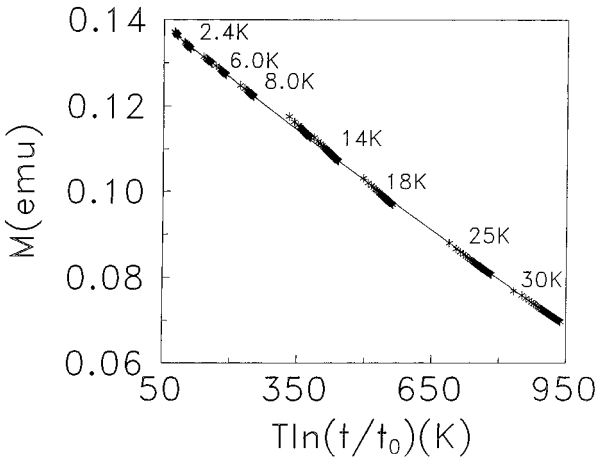

Figure 6. Time-dependent magnetization $M(t)$ vs T ln(t/t_0) for γ-Fe_2O_3 ferrofluid, with $t_0 = 10^{-10}$ s.

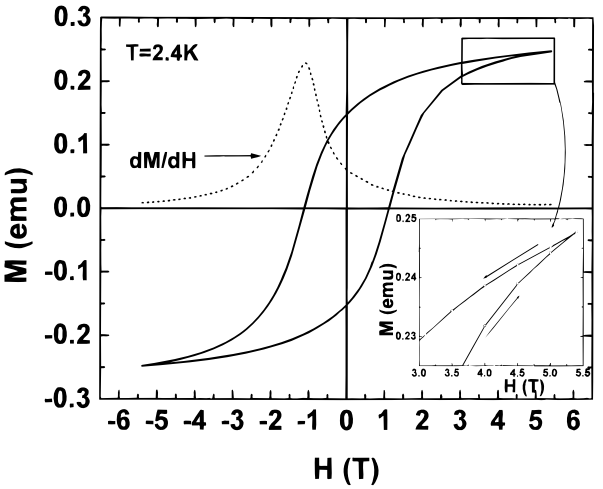

Figure 7. Magnetization versus applied magnetic field obtained at $T = 2.4$ K, for $CoFe_2O_4$ particles. The inset is the high-field region, showing that the loop is not closed, which indicates that the anisotropy field is larger than 5 T.

nanoscale magnetic particles having a low anisotropy field, such as Fe_3O_4.[10,23]

6.3. Nanoscale $CoFe_2O_4$ Particles Dispersed in Water. $CoFe_2O_4$ is an inverse spinel with a very large magnetic anisotropy, $K = 10^7$ erg/cm^3. Therefore, a system formed by mesoscopic particles of this spinel should constitute a well-defined arena in which to observe quantum tunneling processes at temperatures of a few kelvin. In Figure 7, we show the hysteresis loop obtained at 2.4 K. In this figure, one feature that should be noted is the nonclosed loop up to 5 T (see the inset), which indicates that the anisotropy field is not smaller than 5 T. By substituting the value of the anisotropy field, $H_K = 5$ T, of these particles into the theoretical expression giving the crossover temperature, we get that $T_C = 5$ K. The average diameter of the particles we prepared is 30 Å. In Figure 8, we show the ZFC and FC curves obtained under different applied fields. As expected, as the field increases, the blocking temperature shifts to lower temperatures due to the reduction in the barrier heights. The relaxation was measured by cooling the sample from room temperature in a field $H_1 = 0.5$ T, and, after arriving at the target temperature, a new field $H_2 = -0.4$ T was applied.

In Figure 9, we show the magnetization versus time on a logarithmic scale. The extracted values of the

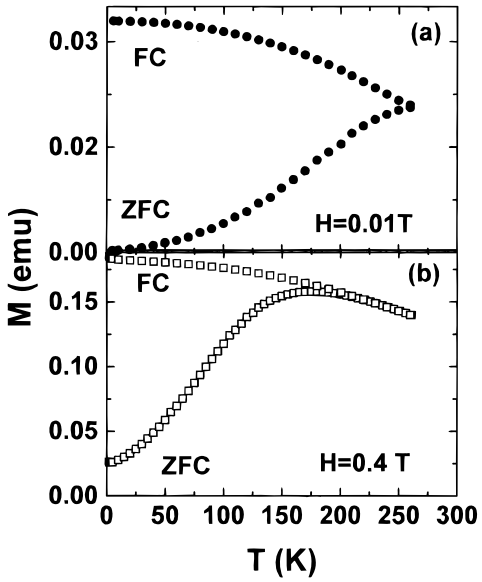

Figure 8. ZFC-FC magnetization curves obtained with different applied field for $CoFe_2O_4$ particles. (a) $H = 0.01$ T, (b) $H = 0.4$ T.

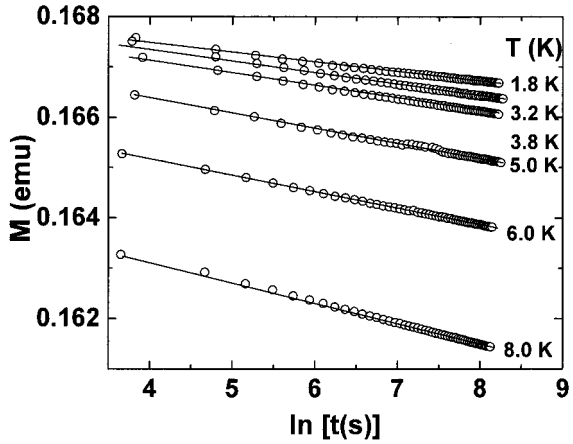

Figure 9. Time decay of magnetization versus ln(t) for different temperatures obtained from $CoFe_2O_4$ particles.

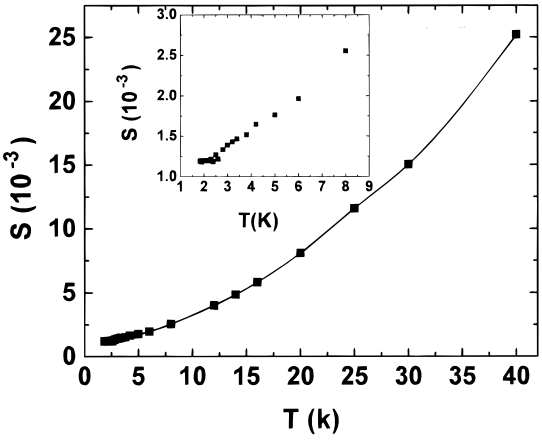

Figure 10. Magnetic viscosity, $S(T)$, extracted from the data shown in Figure 9, versus temperature.

magnetic viscosity are shown in Figure 10. From this figure, it is clear that between 5 and 2.5 K, the viscosity changes linearly with the temperature. These values are extrapolated to zero for $T = 0$ K, which indicates that the interaction between particles is much smaller than the energy barrier height. This is clear, in this

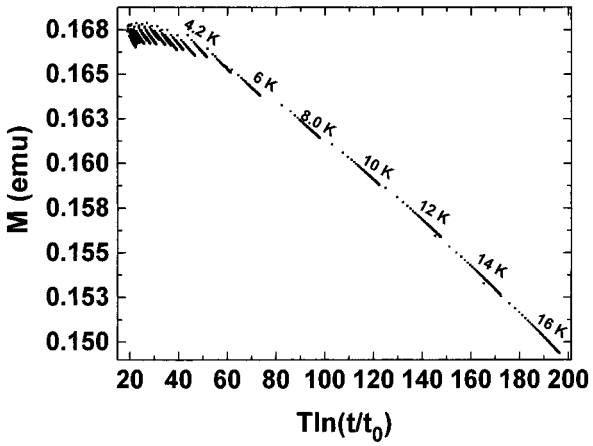

Figure 11. Magnetization obtained in the relaxation process (shown in Figure 9) versus $T \ln(t/t_0)$, with $t_0 = 10^{-10}$ s.

case, because the effective dipole field due to the interaction between particles is much less than 0.01 T and we are dealing with anisotropy barriers corresponding to a field of 5 T. Below 2.5 K, we observe a plateau in the viscosity and that the $M(t)$ data do not scale anymore in the $T \ln(t)$ plot (Figure 11).

The above two experimental observations point toward the occurrence of nonthermal relaxation processes, which is consistent with the fact that, for this high anisotropy material, the low-temperature relaxation is dominated by quantum tunneling out of metastable states rather than by thermal transitions. The experimental crossover temperature of 2.5 K is in agreement with that suggested by theory, 5 K. Very similar results have been obtained in other mesoscopic particles or grains owing to the high magnetic anisotropy.[24−27] The parameters of the materials used in the experiments are summarized in Table 1.

From the table, we may conclude that single domain particles with average volume of 500 nm^3 and anisotropy constant $K \sim 10^6$ erg/cm^3 constitute excellent systems for the study of the occurrence of quantum tunneling processes of magnetization. It also appears that the matrix in which the particles are embedded plays an important role in determining the behavior of the particles. For example, the γ-Fe_2O_3 particles embedded in a silicate matrix exhibit nonthermal relaxation below 2.1 K, while the same particles embedded in sulfonated polystyrene dispersed in water relax thermally to 1 K. Another example of the important role played by the matrix corresponds to the observed dependence of the crossover temperature T_C on the nature of the matrix in which the $CoFe_2O_4$ particles were embedded. These two examples are in agreement with the theoretical prediction[31] that the crossover temperature T_C depends on the Young's modulus of the matrix in which the particles are embedded. The Young's modulus of the matrix should be high enough to allow the conservation of the total angular momentum when the tunneling processes occur. When it is not, tunneling can not occur. However, it is also possible that particles have a different morphology in the different matrices affecting the anisotropy.

Very recently Kodama et al.[24] have given an alternative explanation for the temperature-independent relaxation observed in their $NiFe_2O_4$ nanoparticles in terms of the dynamics of surface spins which behave

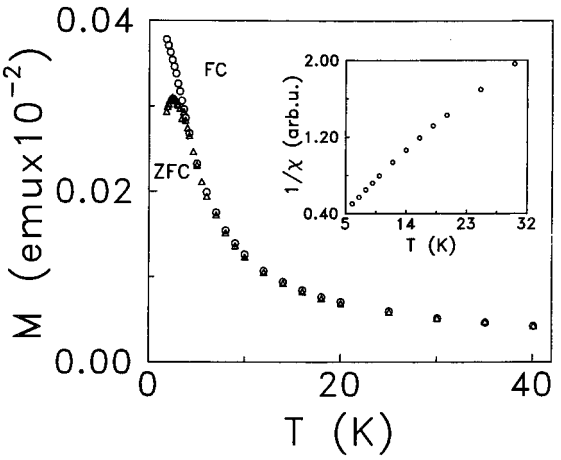

Figure 12. ZFC-FC magnetization for granular system [Cu-(100 Å)/Dy(20 Å)]$_{x30}$ with applied field $H = 0.01$ T.

like a spin-glass with an energy distribution $n(E) \sim 1/E$. This new interpretation could be verified by looking at the magnetic relaxation data, because at low temperature, that is, in the vicinity of the singularity of $n(E)$, the relaxation law should change from the usual ln(t) time dependence to the ln(ln(t)) law explained earlier.[6]

6.4. Mesoscopic Granular Materials. The atomic evaporation of different metals with low miscibility can produce samples composed of very small granular particles. Therefore, very thin films of high-anisotropy rare-earth elements also constitute valuable structures for the study of quantum tunneling of magnetization. This is because the two most important requirements to detect quantum relaxation phenomena, i.e., high magnetic anisotropy and a broad distribution of energy barriers, in this case, may be associated with the broad distribution in the volume of the grains. For example, the evaporation of Dy and Cu produces samples with mesoscopic granular particles of Dy imbedded in a Cu matrix, instead of the usual layered structures. In this section, we show results obtained for two Dy/Cu multilayers of composition [Cu(100 Å)/Dy (40 Å)]$_{x20}$, sample 1, and [Cu(100 Å)/Dy(20 Å)]$_{x30}$, sample 2, respectively, deposited on Kapton.[32] The typical value of the magnetocrystalline anisotropy constant of bulk Dy, 5×10^7 erg/cm^3, suggests that the crossover between the classical and quantum regimes occurs in the kelvin regime.

In these materials, the existence of the ferromagnetic grains, as well as their size distribution, may be unequivocally verified by measuring the ZFC and FC magnetization. The detection of a blocking temperature, which is shifted with the field intensity, and the irreversibility between the ZFC and FC curves below the blocking, are clear indications of the existence of the grains. Moreover, above the blocking temperature, the $M(T)$ data should follow a Curie law.

In Figure 12, we show the ZFC and FC curves for a sample containing a 20 Å thick film of Dy. From the blocking temperature of the two samples, $T_B = 25$ K, sample 1, and $T_B = 2.5$ K, sample 2, we have estimated the average energy barrier, $25\ K_B T_B = U = KV$, of the Dy clusters in the two samples. Taking the value for K that has been experimentally determined from the isothermal $M(H)$ high-field measurements, we got the average activated volume for the two samples, $V_1 = 2000$ Å^3 and $V_2 = 150$ Å^3 for samples 1 and 2, respectively.

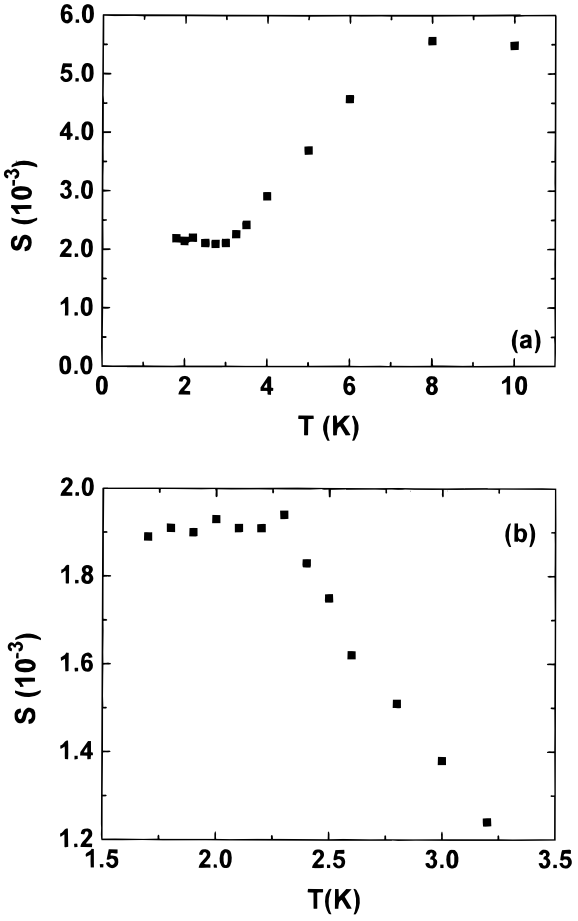

Figure 13. Magnetic viscosity extracted from relaxation measurements obtained at different temperatures with applied field $H_1 = 0.01$ T, and $H_2 = -0.01$ T. (a) Sample [Cu(100 Å)/Dy(40 Å)]$_{x20}$. (b) Sample [Cu(100 Å)/Dy(20 Å)]$_{x30}$. The fact that the plateau in the $S(T)$ data is observed just at the blocking temperature, $T_B = 2.4$ K, should be an indication that the blocking is represented by quantum flipping of the magnetization vector with a lifetime longer than 30 s.

The relaxation of the thermoremanant magnetization for the two samples follows quite well the ln(t) law below the blocking temperature, as we expect in a system with a broad distribution of energy barriers. In Figure 13, we show the magnetic viscosity extracted from the logarithmic decay of the magnetization. The most important features of this figure are (1) $S(T)$ shows a maximum at temperatures $T < T_B$, (2) $S(T)$ decreases as temperature increases above T_B, and (3) $S(T)$ changes its behavior below several kelvin, that is, S is constant at very low temperature.

In sample 1, the blocking occurs at higher temperature than the crossover temperature, indicating that the quantum tunneling of magnetization occurs in the blocked state. In sample 2, the plateau of the viscosity is observed just at the blocking temperature, $T_B = 2.5$ K, which is the evidence that the blocking of the magnetic moments is destroyed by quantum flipping of the magnetization vectors, whose lifetimes range from 10 to 4000 s. Sample 2 enters the quantum regime directly from the classical superparamagnetic regime.

In summary, we note that all the results obtained to date from relaxation experiments show a sharp transition between the two regimes, thermal and quantum, suggesting that dissipation effects in magnetic tunneling are not important. There is also a clear scaling between

the values of the crossover temperature and the magnetic anisotropy constant of the mesoscopic particles. When the applied magnetic field increases, the crossover temperature T_C shifts to lower temperatures, which is in agreement with the fact that T_C scales with the energy barrier height and decreases with the intensity of the magnetic field.

6.5. High-Spin Polynuclear Compounds. We have seen in the previous examples that the systems with a broad distribution of energy barriers always provide us with metastable states whose lifetimes cover a very large time window, which, in principle, can be examined using different techniques. The disadvantage of these systems is that only qualitative comparison can be made with theory due to the statistical nature of the processes. It is important, therefore, to prepare both bulk[33] and mesoscopic magnetic systems having only a single barrier for all metastable states. Very recently, it has been verified that polynuclear compounds meet this requirement.[34] These systems are intermediate between purely paramagnetic molecules and mesoscopic systems; the number of magnetic cations inside each molecule of a polynuclear compound may range from two to more than a dozen, with the cluster having a net magnetic moment of only a few Bohr magnetons.

The most remarkable differences between mesoscopic systems and the high-spin polynuclear compounds relate to the facts that (a) these compounds are composed of identical molecular building blocks, and, consequently, there is an universal anisotropy barrier height, and (b) the two wells associated with the anisotropy barrier contain a discrete spectrum of spin levels of different orientations. This explains why these materials show exponential relaxation and discrete magnetization jumps during the magnetizing process.

We now show some of the recent results that were obtained for these materials and explain the physics underlying the phenomena. The material studied[35] is a molecular crystal of unit formula $Mn_{12}O_{12}(CH_3COO)_{16}(H_2O)_4$. In the crystal, the molecules exist in a tetragonal lattice;[36,37] the net spin is $S = 10$ and is oriented along the c axis. The strong uniaxial magnetic anisotropy of the Mn_{12} molecules suggests that each molecule has, in the absence of an applied magnetic field, a doubly degenerate spin ground state. That is, the different spin levels S_Z ($S_Z = -10, -9, ..., 0, ..., 9, 10$) are degenerate with respect to the absolute value of S_Z and occupy the two wells of the anisotropy barrier. When an external magnetic field is applied, one of the two wells becomes metastable (see cover figure). It has been proposed[35] that the energy of the different spin levels in this system is described by the Hamiltonian

$$H = -DS_Z^2 + g\beta SH \qquad (6)$$

where D is the anisotropy energy constant and H is the applied magnetic field. The solution of this Hamiltonian on the basis of a set of the 21 states $|S,S_Z\rangle$ with $S = 10$, shows that there are certain values for the magnetic field, called crossing fields, in which the spin levels in the two wells have the same energy (see Figure 14). In fact, this occurs at constant intervals of the magnetic field (vide infra).

The results presented here were obtained from a sample in which the c axes of the molecules were oriented in the same direction by an external field.[35] In

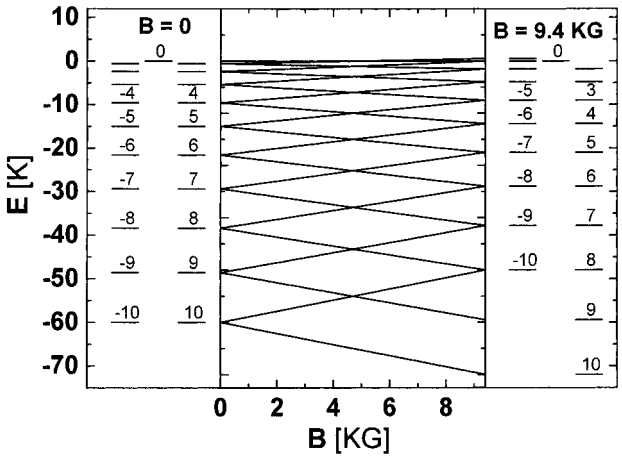

Figure 14. Sketch of crossing of energy levels in two wells as function of applied magnetic field for Mn_{12}.

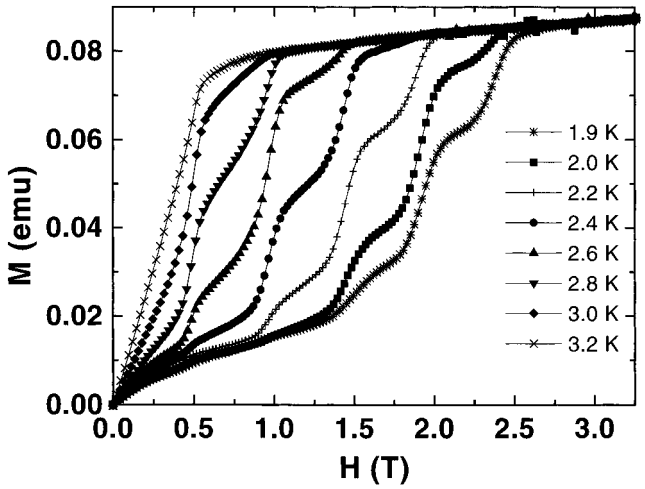

Figure 15. Magnetization as function of applied field obtained at different temperatures, with applied field parallel to the c axis of Mn_{12}.

Figure 15, we show $M(H)$ data, obtained at different temperatures, after zero field cooling of the sample to the measuring temperatures. The jumps in the hysteresis loops appear at constant intervals of the applied magnetic field. The existence of the jumps is well understood in the scope of the above Hamiltonian. As the external applied field increases from zero, the degeneracy of the two wells is broken and the magnetization grows as a consequence of the alignment of the magnetic moments of the molecules along the magnetic field. When the applied field reaches the value of the first crossing field, the resonant tunneling processes occur between the levels of the two wells having the same energy. Consequently, the tunneling leads to a faster variation of the magnetization. By further increasing the external applied field, the system arrives at the next crossing field and new jumps appear.

We have also studied the variation of the relaxation rate with the field at different temperatures. The sample is first zero field cooled, then the field is applied, and the variation of the magnetization with time is detected during 2 h. The relaxation of the magnetization follows quite well the exponential law from which the relaxation rate was extracted (Figure 16). From this figure, it is clear that the jumps in the relaxation rate appear at the same fields as the jumps in the hysteresis loops. Moreover, as the temperature rises, the height

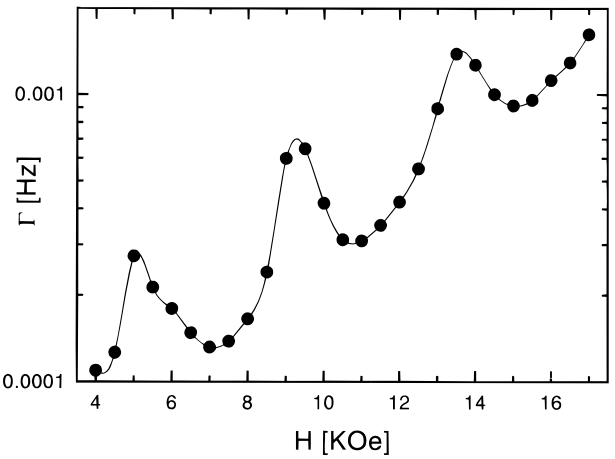

Figure 16. Relaxation rate extracted from the exponential relaxation of magnetization as a function of applied field at $T = 2.2$ K for sample of Mn_{12}.

of the jumps in the relaxation rate increases. This could be interpreted in terms of the occurrence of a thermally assisted resonant tunneling process. When the temperature increases, the levels near the top of the metastable wells are more populated, and, consequently, the relaxation rate increases.

7. Conclusions and Remarks

In conclusion, we have shown that magnetic relaxation studies on nanostructured materials are suitable to detect quantum tunneling processes of the magnetization vector. In the case of single domain particles with broad size distribution, the relaxation law is logarithmic and the magnetic viscosity in the quantum regime is independent of temperature. In the thermal regime, the $S(T)$ data follow very well the theoretical predictions obtained from Monte Carlo simulations and computational models. In the case of an universal energy barrier height, the relaxation is exponential, as has been demonstrated in the Monte Carlo simulations. Having identical magnetic clusters, as found in polynuclear molecules, makes it possible to control all of the variables entering in the quantum problem and to achieve a full correlation between experiment and theory. The existence of a discrete spectrum of spin levels in the anisotropy wells, which correspond to the different possible orientations of the net quantum spin of each molecule, is the origin of the jumps in both the hysteresis loops and relaxation rate. Similar behavior would be expected for nanostructured materials containing single domain particles of uniform size. In closing, we note that the design, synthesis, and characterization of new nanostructured materials will offer further opportunity to elucidate quantum mechanical processes in these materials and lead to the possible discovery of new magnetic and other physical phenomena.

Acknowledgment. J.T. thanks the CICYT and European Community Project No. ERB4050PL930639 for financial support; X.X.Z. thanks the CIRIT de la Generalitat de Catalunya for financial support.

References

(1) Chudnovsky, E. M.; Gunther, L. *Phys. Rev. Lett.* **1988**, *60*, 661. Chudnovsky, E. M.; Gunther, L. *Phys. Rev. B* **1988**, *37*, 9455.
(2) Stamp, P. C. E. *Phys. Rev. Lett.* **1991**, *66*, 2802.
(3) Bean, C. P.; Livingston, J. *J. Appl. Phys.* **1959**, *30*, 120S.
(4) Weil, L. *J. Chim. Phys.* **1954**, *51*, 715.
(5) Caneschi, A.; Gatteschi, D.; Sessoli, R.; Barra, A. L.; Brunel L. C.; Guillot, M. *J. Am. Chem. Soc.* **1991**, *113*, 5873.
(6) Tejada, J.; Zhang, X. X.; Chudnovsky, E. M. *Phys. Rev. B* **1993**, *47*, 14977.
(7) Vincent, E.; Hamman, J.; Prene, P.; Tronc, E. *J. Phys. France* **1994**, *4*, 273.
(8) González- Miranda, J.; Tejada, *J. Phys. Rev. B* **1994**, *49*, 3867. Sánchez, C.; González-Miranda, J. M.; Tejada, J. *J. Magn. Magn. Mater.* **1995**, *140−144*, 365.
(9) Hernández, J. M.; Zhang, X. X.; Tejada, J. *J. Appl. Phys.* **1996**, *79*, 4686.
(10) Tejada, J.; Zhang, X. X.; Balcells, Ll. *J. Appl. Phys.* **1993**, *73*, 6709. Barbara, B.; et al. *J. Appl. Phys.* **1993**, *73*, 6703.
(11) NATO workshop on Quantum Tunneling of the Magnetization; Barbara, B., Gunther, L., Eds.; Kluwer Publishers: Dordrecht, 1995.
(12) Krotenko, E.; Zhang, X. X.; Tejada, J. *J. Magn. Magn. Mater.* **1995**, *150*, 119.
(13) Barbara, B.; Chudnovsky, E. M. *Phys. Lett. A* **1990**, *145*, 205.
(14) Ford, G. C.; Harrison, P. M.; Rice, D. F. W.; Swith, J. M. A.; Treffy, A.; White J. L.; Yoriu, J. *Philos. Trans. R. Soc. London B* **1984**, *304*, 551.
(15) Bell, S. H.; Weir, M. P.; Dickson, D. P. E.; Gibson, J. F.; Sharp, G. A.; Peters, T. T. *Biochim. Biophys. Acta* **1984**, *787*, 227.
(16) Tejada, J.; Zhang, X. X. *J. Phys.: Condens. Matter* **1994**, *6*, 263.
(17) Gider, S.; Awschalom, D. D.; Douglas, T.; Mann, S.; Chaparala, M. *Science* **1995**, *268*, 77. Tejada, J. *Science* **1996**, *272*, 424. Garg, A. *Science* **1996**, *272*, 424. Gider, S.; Awschalom, D. D.; DiVincenzo D. P.; Loss, D. *Science* **1996**, *272*, 425.
(18) Kilcoyne, S. H.; Cywinski, R. *J. Magn. Magn. Mater.* **1995**, *140−144*, 1466.
(19) Landolt-Börstein, New Series, Band 4, Teila; Springer-Verlag: Berlin, 1970.
(20) Ziolo, R. F.; et al. *Science* **1992**, *257*, 219.
(21) Ziolo, R. F. 1st Int. Conf. on Nanostructured Materials, Cancun, Mexico, Sept. 21−26, 1992. Ziolo, R. F. NATO Advanced Study Institute on Nanophase Materials, Corfu, Greece, June 20−July 2, 1993.
(22) Zhang, X. X.; Ziolo, R. F.; Kroll, E. C.; Bohigas, X.; Tejada, J. *J. Magn. Magn. Mater.* **1995**, *140−145*, 1853.
(23) Tejada, J.; et al. *J. Appl. Phys.* **1993**, *73*, 6952.
(24) Kodama, R. H.; Seaman, C. L.; Berkowitz, A. E.; Mapple, B. *J. Appl. Phys.* **1994**, *75*, 5639. Kodama, R. H.; Berkowitz, A. E.; McNiff, E. J., Jr.; Foner, S., preprint, 1996.
(25) Paulsen, C.; Sampaio, L. C.; Barbara, B.; Tucoulu-Tachoneres, R.; Fruchart, D.; Marchand, A.; Tholence, J. L.; Uehara, M. *Europhys. Lett.* **1992**, *19*, 643.
(26) Ibrahim, M. M.; Darwish, S.; Seehra, M. M. *Phys. Rev. B* **1995**, *51*, 2955.
(27) Balcells, L. L.; et al. *Z. Phys. B: Condens. Matter* **1992**, *89*, 209.
(28) Zhang, X. X.; Hernandez, J. M.; Tejada, J.; Ziolo, R. F. *Phys. Rev. B*, in press.
(29) Zhang, X. X.; Tejada, J. *J. Appl. Phys.* **1994**, *75*, 5637.
(30) Zhang, X. X.; Tejada, J., unpublished.
(31) Chudnovsky, E. M. *Phys. Rev. Lett.* **1994**, *72*, 3433.
(32) Tejada, J.; Zhang, X. X.; Ferrater, C. *Z. Phys. B* **1994**, *94*, 245.
(33) Tejada, J.; Zhang, X. X.; Roig, A.; Nikolov, O.; Molins, E. *Europhys. Lett.* **1995**, *30*, 227.
(34) Paulsen, C.; Park, J. G.; Barbara, B.; Sessoli, R.; Caneschi, A. *J. Magn. Magn. Mater.* **1995**, *140−144*, 1891.
(35) Friedman, J. R.; Sarachik, M. P.; Tejada, J.; Maciejewski, J.; Ziolo, R. F. *Phys. Rev. Lett.* **1996**, *76*, 3830. Hernández, J. M.; Zhang, X. X.; Tejada, J.; Friedman, J. R.; Sarachik, M. P.; Maciejewski, J.; Ziolo, R. F., to be published.
(36) Novak, M. A.; Sessoli, R. *NATO Workshop on Quantum Tunneling of the Magnetization*; Barbara, B., Gunther, L., Eds.; Kluwer Publishers: Dordrecht, 1995.
(37) Lis, T.; Jezowska-Trzebiatowska, B. *Acta Crystallogr.* **1977**, *B33*, 2112.

CM9602003